Shortened Finite Geometry LDPC Codes with 5 to 15 per cent Code Overhead for Fiber Optic Communications

Tobias Rankl, Matthias Breuninger, Klaus Oestreich

Abstract **For high speed fiber optical communications Low-Density Parity-Check (LDPC) codes with code overhead between 5 and 15% are of great interest. We focus on Euclidean and projective geometry LDPC codes and present a large number of them with the mentioned overhead. Further the bit error rate perfomance (BER) of some of the presented codes is compared using an iterative soft-in soft-out sum product algorithm (SPA) decoder and a two-stage hybrid decoder.**

Keywords **LDPC codes, Optical communication**

1. Introduction

The development of high speed fiber optic data communication towards 100 Gbit/s Ethernet and beyond requires powerful forward error correction (FEC) in order to achieve an almost error free data throughput. At present limited speed of the applied semiconductor technology is an obstacle for the implementation of FEC codes. To overcome this problem FEC codes are attractive, which can be implemented by parallel structures. Reed Solomon codes, finite geometry Low-Density Parity-Check (LDPC) codes as well as some others exhibit this potential. In this paper we focus on quasi-cyclic (QC) finite geometry LDPC codes with high code rates.

LDPC codes that are based on Euclidean and projective geometries were recently developed [1, 2] and investigated for fiber optic transmission links [3, 4, 5, 6, 7]. Many authors focus on the construction principles of these codes. In order to demonstrate the lage variety of LDPC codes that can be obtainded by this approach we present a set of codes with overhead between 5% and 15%. Several of them provide a good compromize with respect to coding performance and complexity. These codes are therefore well suited for high speed fiber optic communications. For comparison code overhead of about 6.7% is also selected that matches with of the widely used Reed Solomon (RS) code RS(255,239) that is described in the ITU-T G.975 recommendation.

We enlarge the number of codes by shortening the base codes which are constructed using Euclidean and projective geometry.[1] Further codes are achieved by applying row and column decomposition. From the resulting large number of codes we select some with specific code rates to demonstrate their bit error rate performance (BER).

This paper is organized as follows. Section 2 provides a brief overview of finite geometry LDPC codes, and the code shortening technique. The optical transmission link and the decoding algorithms are presented in Section 3. In Section 4 the performance of the proposed codes is demonstrated by computer simulations and Section 5 concludes the paper.

2. Shortened Finite Geometry LDPC Codes

LDPC codes are a subset of linear block codes. It has been shown that these codes can achieve a BER performance with iterative decoding that is close to the channel capacity [8]. LDPC codes are specified by their parity check matrix $\boldsymbol{H}$. With the generator matrix $\boldsymbol{G}$, which is necessary for encoding, the condition $\boldsymbol{G}\boldsymbol{H}^T = \boldsymbol{0}$ has to be fulfilled. If the information word is of length k, and the codeword of length n, the code rate is

$$R_c = \frac{k}{n} \tag{1}$$

which yields the overhead

$$O_c = \frac{n-k}{k} = \frac{1}{R_c} - 1. \tag{2}$$

$\boldsymbol{H}$ is of size $(J \times n)$, where J is the number of parity check equations of the code.

The construction of finite geometry LDPC codes is based on lines and points of m-dimensional Euclidian and projective geometries over finite fields. As a result four different classes of finite geometry LDPC codes can be obtained: Type 1 and type 2 Euclidean geometry (EG) LDPC codes as well as type 1 and type 2 projective geometry (PG) LDPC codes. Type 2 codes are derived from the type 1 codes by transposing their parity-check matrix.

Each row of $\boldsymbol{H}$ consists of ρ 1's and each column comprises γ 1's.The remaining elements of $\boldsymbol{H}$ are 0. The row weight ρ and column weight γ are small compared to the length n of the code and the number of rows in $\boldsymbol{H}$. Thus, the parity check matrix has a low density of 1's. In general the type 2 EG and PG LDPC codes are not cyclic but can be put in quasi-cyclic (qc) form. Matrix $\boldsymbol{H}_{\mathrm{qc}}$ of a qc code consists of $c = n/J$ columns of circulant submatrices, where n has to be an integer multiple of J. An example of a quasi-cyclic parity check matrix is shown in eq. (3) for a structured LDPC code of EG type 2 with $m = 2$, $s = 1$ and 3 submatrices, where m and s describe the geometry according to [1] e.g. $EG\,(m, 2^s)$ stands for an

[1] The codes that arise out of a base code shortening, are of various codeword length and code rates. Not all of them are sufficiently long or of high code rate.

Dipl.-Ing. T. Rankl, Dipl.-Ing. M. Breuninger, Dipl.-Ing. K. Oestreich, University of Stuttgart, Institute for Telecommunications, Pfaffenwaldring 47, D-70568 Stuttgart, Germany.

m-dimensional Euclidian geometry over the Galois field $GF(2^s)$.

$$\boldsymbol{H}_{\mathrm{qc}} = \left[\begin{array}{ccccccc|ccccccc|ccccccc} 1&0&0&0&1&0&0&1&1&0&0&0&0&0&1&0&1&0&0&0&0\\ 0&1&0&0&0&1&0&0&1&1&0&0&0&0&0&1&0&1&0&0&0\\ 0&0&1&0&0&0&1&0&0&1&1&0&0&0&0&0&1&0&1&0&0\\ 1&0&0&1&0&0&0&0&0&0&1&1&0&0&0&0&0&1&0&1&0\\ 0&1&0&0&1&0&0&0&0&0&0&1&1&0&0&0&0&0&1&0&1\\ 0&0&1&0&0&1&0&0&0&0&0&0&1&1&1&0&0&0&0&1&0\\ 0&0&0&1&0&0&1&1&0&0&0&0&0&1&0&1&0&0&0&0&1 \end{array}\right] \tag{3}$$

The codes derived in this paper are a subset of the class of shortened finite geometry LDPC codes that are introduced in [1], and are of type 2. They can be systematic and not.

2.1 Shortening of LDPC codes

Based on the presented type 2 parity check matrices $\boldsymbol{H}_{\mathrm{qc}}$ new parity check matrices and consequently new codes can be created by shortening the original code. This is done by deleting columns in $\boldsymbol{H}_{\mathrm{qc}}$. For $m > 2$ the $J \times n$ EG or PG parity check matrix $\boldsymbol{H}_{\mathrm{qc}}$ of type 2 consists of $c = n/J > 1$ columns of circulant $J \times J$ matrices and describes a quasi cyclic code. To maintain the quasi cyclic property complete circulant $J \times J$ submatrices can be deleted. If $t < c$ circulant submatrices are deleted, and if systematic encoding is applied, then the new parity check matrix specifies a quasi cyclic $(n - J\,t, n - J\,(t+1))$ code with the code rate $R_c = 1 - 1/(c-t)$. The column weight γ remains the same, and the row weight ρ is reduced to $\rho = \gamma\,(c-t)$.

2.2 Proposed LDPC codes for optical communications

In the following, we present a variety of finite geometry codes with various code parameters. Table 2 shows base-codes. G indicates the geometry and c is the number of matrices. For all codes the length of the codeword n and the information word k, the code rate R_c, the overhead O_c, the row weight ρ as well as the column weight γ and the number of parity check equations J are given. The LDPC codes presented in the tables 3 to 9 are derived from the base-codes by use of column splitting. Their overhead exhibits the values $5\%, 6.7\%, 7.5\%, 10\%, 12.5\%, 14.3\%$ and 15%. Both systematic and non-systematic codes are given. These tables show the manifold properties of the codes that can be derived from the Euclidean and projective geometry LDPC base-codes.

The codes given in tables 3 - 9 present just a subset of structured finite geometry codes. Other codes with various code rates can be obtained by applying row and column decomposition to the parity check matrices, where each circulant submatrix is split into several circulant submatrices. By this way extended finite geometry LDPC codes of nearly any code rate can be generated. Table 10 shows several examples.

3. System Model and Decoding

Fig. 1 shows the block diagram of a fiber optic transmission link with forward error correction. The sequence of information bits b_k is encoded and mapped into the code symbols a_m with code rate R_c. a_m is then transmitted. The sampled sequence at he output of this transmission link consists of q_m. This sequence is decoded either by a soft-in hard-out (SIHO) or by a soft-in soft-out (SISO) decoder to obtain the decoded sequence $\widehat{a}_m$. As SISO the sum product algorithm (SPA) decoder or as SIHO a two-stage hybrid SPA-majority logic (MLG) decoder can be applied. Finally, an inverse encoding operation is performed on $\widehat{a}_m$, yielding the bit estimates $\widehat{b}_k$.

Section ① - ② in Fig. 1 represents the optical transmission link. Intensity modulation (IM) and non return to zero (NRZ) impulse shaping is used as a transmission format. An externally modulated optical transmitter (TX) and an optically preamplified direct detection receiver (RX) is used. The RX consists of an erbium doped fiber amplifier (EDFA), an optical filter, a photo diode and an electrical filter. A single mode fiber is assumed as transmission medium. The system configuration is taken from [5], where a detailed mathematical model of ① - ② is also given.

3.1 Decoder

Due to the high data rates of multiples of 10 Gbit/s per channel real-time decoding algorithms and hardware implementations are a great challenge. Promising solutions are the SPA and hybrid decoders. Both decoding methods can be applied for the described LDPC codes.

The decoding consists of two different operations. First, the error correction operation is performed by the mentioned algorithms such as SPA or a two stage hybrid decoding. Secondly, a conversion of the codeword to the desired information sequence is done by an inverse encoder. In the following sections these operations are described in more detail.

3.1.1 The sum product algorithm decoder

The SISO decoder with iterative sum product algorithm [9] uses the channel log likelihood ration (LLR) $L_{ch}\,(a_m|\,q_m)$ as input which is given by

$$L_{ch}\,(a_m|\,q_m) = ln\frac{\sum_{\forall\,\vec{a}_{[m]}} p\,(\,q_m|\,a_m = 0, \vec{a}_{[m]})}{\sum_{\forall\,\vec{a}_{[m]}} p\,(\,q_m|\,a_m = 1, \vec{a}_{[m]})}. \tag{4}$$

In this equation $p\,(\,q_m|\,\vec{a})$ is the conditional probability density function of q_m which describes the statistical properties of the channel output if the bit pattern $\vec{a}$ was transmitted. $\vec{a}_{[m]}$ is obtained from $\vec{a}$ by ignoring mth component a_m. The derivation of $p\,(\,q_m|\,\vec{a})$, $\vec{a}$ and $\vec{a}_{[m]}$ can be found in [5].

The sum product algorithm is based on the Tanner graph [9]. In each iteration information is passed between the variable- and the checknodes. Every node offers a calculation rule in order to combine the incomming information. Thus the reliability of each bit of the codeword can

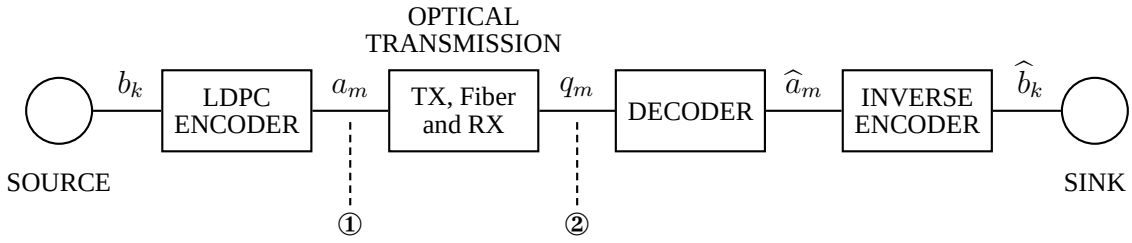

Fig. 1. Block diagram of system model with LDPC encoder and decoder.

be improved from one iteration to the next. The performance of the algorithm depends very much on cycles of short length in its Tanner graph. Such cycles result in a high correlation between successive decoding iterations. Suitable LDPC codes should not contain cyles of length 4 and only few cyles of length 6.

The SPA decoding requires real number addition, substraction, multiplication, division, and exponential as well as logarithm operations. Thus this decoder exhibits a large hardware complexity but offers a very good error correction performance. Due to its potential for parallelization, it is well suited for real time implementation at high speeds.

3.1.2 The two-stage hybrid decoder

The two-stage hybrid decoder [1] consists of a serial concatenation of an SPA decoder that performs two iterations, a hard decision devise, and a majority logic (MLG) decoder. The hard decision operates on the LLR, and a decision threshold of zero (a LLR value equal to 0 corresponds to a probability of 0.5).

MLG decoding is a simple and effective hard-in hard-out (HIHO) scheme for decoding of cyclic and quasi cyclic block codes [9]. MLG decoding is based on orthogonal parity check sums within the parity check matrix $\boldsymbol{H}_{\mathrm{qc}}$. For every bit position l there is a set of rows in $\boldsymbol{H}_{\mathrm{qc}}$ which are orthogonal on this bit postion. The lth symbol of each row in this set is 1 and not any two rows have a 1 in any other position in common. This orthogonality property is fulfilled if the code has no cycles of length 4. The finite geometry LDPC codes in Tabels 2 - 10 exhibit this property, and therefore they can be decoded by an one step MLG decoder.

A multitude of one step MLG decoder implementations can be found in [9]. In most cases they are based on a simple shift register and a majority logic gate. Based on the number of errors, indicated by the parity check equations, the majority logic gate decides whether the considered symbol is correct or not. Due to the simplicity of this decoding method, and the large parallelization potential, high speed hardware implementations are possible.

The serial concatenation of SPA with only 2 iterations and the MLG decoder combines low latency decoding with a relatively good performance. In comparision a general SPA decoder requires a larger number of iterations and exhibits therefore a high latency.

3.1.3 The inverse encoder

The inverse encoder in Fig. 1 is required to obtain the information sequence. In case of a systematic code this operation is simple, because the codeword contains the information word separated from the coded bits. However for a non-systematic code information bits and coded bits are not separated. Therefore, an operation, which is inverse to encoding has to be performed. This can be implemented as a division of the codeword by the generator polynomial which can be implemented rather easily. This holds only for cyclic and quasi cyclic block codes. [2]

4. Performance of proposed LDPC Codes

We present the bit error rate (BER) performance of some of the LDPC codes listed in tables 3 to 9. The communication link in Fig. 1 exhibits a fixed net bit rate of $R_b = 10\,\mathrm{Gbit/s}$, a differential group delay of $\Delta\tau = 60\,\mathrm{ps}$ due to polarization mode dispersion and a chromatic dispersion of $R_D = 400\,\mathrm{ps/nm}$. All investigated LDPC codes are summarized in Table 1. For the sake of simplicity a short notation of the codes is chosen. E.g. EG2m3s3-8of9-ext indicates the extended EG-2 code with $m = 3$, $s = 3$ and 8 of 9 submatrizes. For all selected LDPC codes the number of cycles of length six in the Tanner graph are given in table 1.

Table 1. Simulated codes and their properties.

Code	n	R_c	γ	cycles of length 6
EG2m6s1-16of31	1008	0.938	2	5439
EG2m7s1-16of63	2032	0.938	2	6096
EG2m8s1-16of127	4080	0.938	2	9690
PG2m8s1-16of85	8176	0.938	3	127239
EG2m5s2-16of85	16238	0.938	4	1145760
EG2m5s2-32of85-ext	32736	0.938	4	272203
EG2m3s3-8of9	4088	0.875	8	14722932
EG2m3s3-8of9-ext	8176	0.875	4	121107
PG2m8s1-8of85	4088	0.875	3	17885

[2] The encoding in this case can be done by a multiplication of generator polynomial and information word. A hardware implementation just consists of a simple shift register operation.

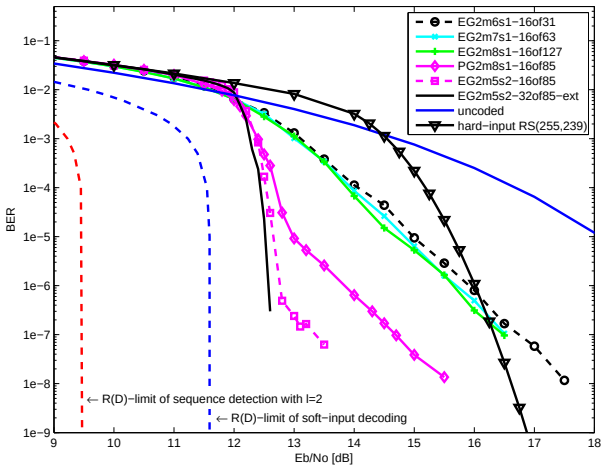

Fig. 2. BER vs. E_b/N_0 for various LDPC codes of Section 2 with $R_c = 0.938$. Various codeword lengths are compared.

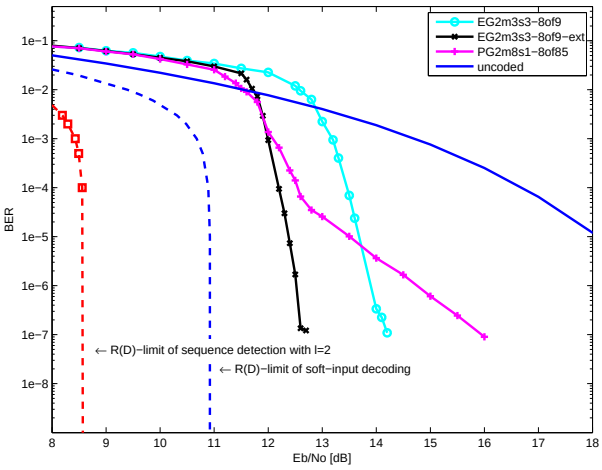

Fig. 3. BER vs. E_b/N_0 chart with comparison of various LDPC codes of Section 2 with $R_c = 0.875$. Extended vs. not extended code.

Fig. 2 shows the BER over E_b/N_0, where E_b is the energy per bit, and N_0 is the total noise spectral density. The chart compares LDPC codes of different lenghts, and a code rate of R_c = 0.938. SPA decoding with 25 iterations is applied.

The performance of a RS(255,239) code, an uncoded transmission, as well as the $R(D)$-limits of soft-input decoding and of sequence detection with two samples per symbol interval are shown as a reference. The $R(D)$-limit of sequence detection indicates the lower bound of electronic signal detection. The $R(D)$-limit of soft-input decoding represents the theoretical SNR-bound of a soft-input decoder respectively.

As can be seen, the codes perform quite differently. The first three codes in Table 1 exhibit a short length and therefore provide lower performance. For a BER $< \ 10^{-9}$, which is required in optical communications, the RS-code outperforms these three codes. As can be seen, longer codes show a steeper turbo cliff, but do not necessarily prevent error floors. The extended EG-2 m = 5, s = 2 code exhibits the best performance, which is only 1 dB from its $R(D)$-limit.

As can be seen in Fig. 3 several extended finite-geometry LDPC codes perform very well with SPA decoding. Column and row extension of the EG-2 m = 3, s = 3 code yields a gain of about 1.5 dB compared to the not extended EG-2 m = 3, s = 3 code. This is due to the fact, that this extension of the code decreases the number of cycles of length six in the Tanner graph by a factor greater than 120. The hardware complexity just stays the same.

Column and row splitting do not result in better performance for all LDPC decoders under consideration. As can be seen in Fig. 4, the extended EG-2 m = 5, s = 2 code just shows the same performance as the not extended code using a two-stage hybrid decoder. The number of cycles of length six is not relevant for this hybrid decoder, as the cycles are not closed within two iterations. For both codes the SPA decoder performs better than the hybrid decoder.

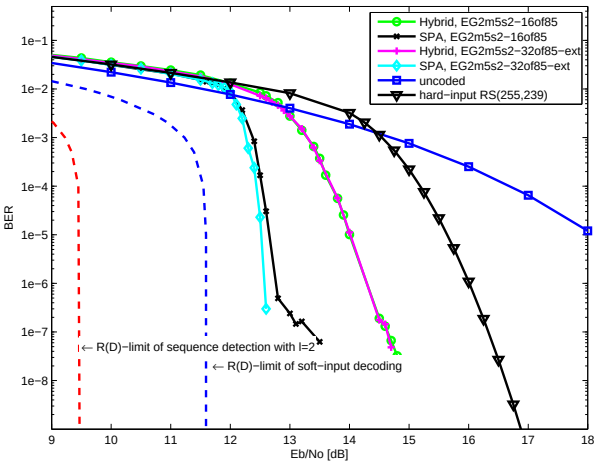

Fig. 4. BER vs. E_b/N_0 chart with comparison of various LDPC codes of Section 2 with $R_c = 0.938$. SPA and hyprid decoding are compared for two different codes.

5. Conclusion

In this paper quasi cyclic LDPC codes with code overhead between 5% and 15% are presented. Shortening of the base codes as well as column and row extension yields to a large set of codes. Due to the variety of properties, this code collection is of interest for different applications, such as high speed optical data transmission, turbo equalization and optical orthogonal frequency division multiplexing. The tabulation gives an insight into manifold characteristics of the LDPC codes belonging to the class of structured finite geometry codes, that are based on Euclidean and projective geometries.

Because of the quasi cyclic property, each code develops a uniform structure within its parity check matrix or equivalently within its Tanner graph. These structures are

highly beneficial for the development of simple and high speed hardware implementations of LDPC decoders.

BER as a function of signal-to-noise ratio (E_b/N_0) is given for various LDPC codes and compared with the respective rate distortion limits. Two different decoding algorithms are applied, namely the powerful sum product algorithm (SPA) decoder and a two-stage hybrid decoder consisting of SPA and majority logic (MLG) decoder. The hybrid decoder provides a good compromise between decoding performance and hardware implementation complexity, and is therefore of interest for optical communications. This also holds for the SPA decoder, as it exhibits a very good performance for selected LDPC codes.

References

[1] Kou, Y.; Lin, S.; Fossorier, M. P. C.: Low-density parity-check codes based on finite geometries: A rediscovery and new results. IEEE Transactions on Information Theory **47** (November 2001), 2711–2735.

[2] Vasic, B.; Milenkovic, O.: Combinatorial constructions of low-density parity-check codes for iterative decoding. IEEE Transactions of Information Theory **50** (June 2004), 1156 – 1176.

[3] Rankl, T.: Turbo equalization with convolutional and LDPC codes as well as analytically computed metrics. April 2008. 9. ITG-Fachtagung Photonische Netze. 165 – 172.

[4] Bülow, H.; Rankl, T.: Soft coded modulation for sensitivity enhancement of coherent 100-Gbit/s transmission systems. Conference on Optical Fiber Communication - incudes post deadline papers, 2009, March 2009. 1 – 3.

[5] Rankl, T.; Kurz, C.; Speidel, J.: Performance bounds of optical receivers with electronic detection and decoding. Journal of Lightwave Technology **27** (August 2009), 3567–3579.

[6] Sahuguede, S.; Julien-Vergonjanne, A.; Cances, J.-P.: Soft decision LDPC decoding over chi-square based optical channels. Journal of Lightwave Technology **27** (August 2009), 3540–3545.

[7] Djordjevic, I. B.; Arabaci, M.; Minkov, L.: Next generation FEC for high-capacity communication in optical transport networks. Journal of Lightwave Technology **27** (Augsut 2009), 3518–3530.

[8] Chung, S.; Forney Jr., G. D.; Richardson, T. J.; Urbanke, R.: On the design of low-density parity-check codes within 0.0045 dB of the Shannon limit. IEEE Communications Letters **5** (Febuary 2001), 58 – 60.

[9] Lin, S.; Daniel J. Costello, J.: Error control coding. Prentice Hall, 2005.

Table 2. EG and PG LDPC base codes of type 2.

G	m	s	n	k	$n-k$	R_c	O_c	c	ρ	γ	J
					EG						
EG-2	5	1	465	435	30	0.935	6.9%	15	30	2	31
EG-2	6	1	1953	1891	62	0.968	3.3%	31	62	2	63
EG-2	7	1	8001	7875	126	0.984	1.6%	63	126	2	127
EG-2	8	1	32385	32131	254	0.992	0.8%	127	254	2	255
EG-2	4	2	5355	5121	234	0.956	4.6%	21	84	4	255
EG-2	5	2	86955	85963	992	0.989	1.2%	85	340	4	1023
EG-2	3	3	4599	4227	372	0.919	8.8%	9	72	8	511
EG-2	3	4	69615	66897	2718	0.961	4.1%	17	272	16	4095
EG-2	4	3	298935	295246	3689	0.988	1.2%	73	584	8	4095
					PG						
PG-2	5	1	630	573	57	0.910	9.9%	10	30	3	63
PG-2	6	1	2667	2547	120	0.955	4.7%	21	62	3	127
PG-2	7	1	10710	10463	247	0.977	2.4%	42	126	3	255
PG-2	8	1	43435	42933	502	0.988	1.2%	85	254	3	511
PG-2	4	2	5797	5501	296	0.949	5.4%	17	84	5	341
PG-2	5	2	92820	91531	1289	0.986	1.4%	68	340	5	1365
PG-2	3	3	4680	4279	401	0.914	9.4%	8	72	9	585
PG-2	3	4	69904	67103	2801	0.960	4.2%	16	272	17	4369
PG-2	4	3	304265	300174	4091	0.987	1.4%	65	584	9	4681

Table 3. Shortened type 2 EG and PG LDPC codes of about 5% overhead (systematic and non-systematic).

G	m	s	n	k	$n-k$	R_c	O_c	c	ρ	γ	J
					systematic codes						
EG-2	6	1	1323	1260	63	0.952	5.0%	21	42	2	63
EG-2	7	1	2667	2540	127	0.952	5.0%	21	42	2	127
EG-2	4	2	5355	5100	255	0.952	5.0%	21	84	4	255
EG-2	5	2	21483	20460	1023	0.952	5.0%	21	84	4	1023
PG-2	6	1	2667	2540	127	0.952	5.0%	21	63	3	127
PG-2	7	1	5355	5100	255	0.952	5.0%	21	63	3	255
PG-2	8	1	10731	10220	511	0.952	5.0%	21	63	3	511
PG-2	5	2	28665	27300	1365	0.952	5.0%	21	105	5	1365
					non-systematic codes						
EG-2	7	1	2667	2541	126	0.953	5.0%	21	42	2	127
EG-2	8	1	5355	5101	254	0.953	5.0%	21	42	2	255
EG-2	3	4	57330	54612	2718	0.953	5.0%	14	224	16	4095
EG-2	4	3	77805	74116	3689	0.953	5.0%	19	152	8	4095
PG-2	6	1	2540	2420	120	0.953	5.0%	20	60	3	127

Table 4. Shortened type 2 EG and PG LDPC codes of about 6.7% overhead (systematic and non-systematic).

G	m	s	n	k	$n-k$	R_c	O_c	c	ρ	γ	J
systematic codes											
EG-2	6	1	1008	945	63	0.938	6.7%	16	32	2	63
EG-2	7	1	2032	1905	127	0.938	6.7%	16	32	2	127
EG-2	8	1	4080	3825	255	0.938	6.7%	16	32	2	255
EG-2	4	2	4080	3825	255	0.938	6.7%	16	64	4	255
EG-2	5	2	16368	15345	1023	0.938	6.7%	16	64	4	1023
EG-2	3	4	65520	61425	4095	0.938	6.7%	16	256	16	4095
EG-2	4	3	65520	61425	4095	0.938	6.7%	16	128	8	4095
PG-2	6	1	2032	1905	127	0.938	6.7%	16	48	3	127
PG-2	7	1	4080	3825	255	0.938	6.7%	16	48	3	255
PG-2	8	1	8176	7665	511	0.938	6.7%	16	48	3	511
PG-2	4	2	5456	5115	341	0.938	6.7%	16	80	5	341
PG-2	5	2	21840	20475	1365	0.938	6.7%	16	80	5	1365
PG-2	3	4	69904	65535	4369	0.938	6.7%	16	272	17	4369
PG-2	4	3	74896	70215	4681	0.938	6.7%	16	144	9	4681
non-systematic codes											
EG-2	6	1	1008	946	62	0.938	6.6%	16	32	2	63
EG-2	7	1	2032	1906	126	0.938	6.6%	16	32	2	127
EG-2	8	1	4080	3826	254	0.938	6.6%	16	32	2	255
PG-2	6	1	1905	1785	120	0.937	6.7%	15	45	3	127
PG-2	4	2	4774	4478	296	0.938	6.6%	14	70	5	341
PG-2	5	2	20475	19186	1289	0.937	6.7%	15	75	5	1365
PG-2	4	3	65534	61443	4091	0.938	6.7%	14	126	9	4681

Table 5. Shortened type 2 EG and PG LDPC codes of about 7.5% overhead (systematic and non-systematic).

G	m	s	n	k	$n-k$	R_c	O_c	c	ρ	γ	J
non-systematic codes											
EG-2	5	1	434	404	30	0.931	7.4%	14	28	2	31
EG-2	6	1	882	820	62	0.930	7.6%	14	28	2	63
EG-2	7	1	1778	1652	126	0.929	7.6%	14	28	2	127
EG-2	5	2	14322	13330	992	0.931	7.4%	14	56	4	1023
EG-2	4	3	53235	49546	3689	0.931	7.4%	13	104	8	4095
PG-2	7	1	3570	3323	247	0.931	7.4%	14	42	3	255
PG-2	8	1	7154	6652	502	0.930	7.5%	14	42	3	511

Table 6. Shortened type 2 EG and PG LDPC codes of about 10% overhead (systematic and non-systematic).

G	m	s	n	k	$n-k$	R_c	O_c	c	ρ	γ	J
systematic codes											
EG-2	5	1	341	310	31	0.909	10.0%	11	22	2	31
EG-2	6	1	693	630	63	0.909	10.0%	11	22	2	63
EG-2	7	1	1397	1270	127	0.909	10.0%	11	22	2	127
EG-2	8	1	2805	2550	255	0.909	10.0%	11	22	2	255
EG-2	4	2	2805	2550	255	0.909	10.0%	11	44	4	255
EG-2	5	2	11253	10230	1023	0.909	10.0%	11	44	4	1023
EG-2	3	4	45045	40950	4095	0.909	10.0%	11	176	16	4095
EG-2	4	3	45045	40950	4095	0.909	10.0%	11	88	8	4095
PG-2	6	1	1397	1270	127	0.909	10.0%	11	33	3	127
PG-2	7	1	2805	2550	255	0.909	10.0%	11	33	3	255
PG-2	8	1	5621	5110	511	0.909	10.0%	11	33	3	511
PG-2	4	2	3751	3410	341	0.909	10.0%	11	55	5	341
PG-2	5	2	15015	13650	1365	0.909	10.0%	11	55	5	1365
PG-2	3	4	48059	43690	4369	0.909	10.0%	11	187	17	4369
PG-2	4	3	51491	46810	4681	0.909	10.0%	11	99	9	4681
non-systematic codes											
EG-2	8	1	2805	2551	254	0.909	10.0%	11	22	2	255
EG-2	4	2	2550	2316	234	0.908	10.1%	10	40	4	255
EG-2	3	3	4088	3716	372	0.909	10.0%	8	64	8	511
PG-2	3	4	30583	27782	2801	0.908	10.1%	7	119	17	4369

Table 7. Shortened type 2 EG and PG LDPC codes of about 12.5% overhead (systematic and non-systematic).

G	m	s	n	k	$n-k$	R_c	O_c	c	ρ	γ	J
systematic codes											
EG-2	5	1	279	248	31	0.889	12.5%	9	18	2	31
EG-2	6	1	567	504	63	0.889	12.5%	9	18	2	63
EG-2	7	1	1143	1016	127	0.889	12.5%	9	18	2	127
EG-2	8	1	2295	2040	255	0.889	12.5%	9	18	2	255
EG-2	4	2	2295	2040	255	0.889	12.5%	9	36	4	255
EG-2	5	2	9207	8184	1023	0.889	12.5%	9	36	4	1023
EG-2	3	3	4599	4088	511	0.889	12.5%	9	72	8	511
EG-2	3	4	36855	32760	4095	0.889	12.5%	9	144	16	4095
EG-2	4	3	36855	32760	4095	0.889	12.5%	9	72	8	4095
PG-2	6	1	1143	1016	127	0.889	12.5%	9	27	3	127
PG-2	7	1	2295	2040	255	0.889	12.5%	9	27	3	255
PG-2	8	1	4599	4088	511	0.889	12.5%	9	27	3	511
PG-2	4	2	3069	2728	341	0.889	12.5%	9	45	5	341
PG-2	5	2	12285	10920	1365	0.889	12.5%	9	45	5	1365
PG-2	3	4	39321	34952	4369	0.889	12.5%	9	153	17	4369
PG-2	4	3	42129	37448	4681	0.889	12.5%	9	81	9	4681
non-systematic codes											
EG-2	7	1	1143	1017	126	0.890	12.4%	9	18	2	127
EG-2	8	1	2295	2041	254	0.889	12.4%	9	18	2	255
EG-2	3	4	24570	21852	2718	0.889	12.4%	6	96	16	4095

Table 8. Shortened type 2 EG and PG LDPC codes of about 14.3% overhead (systematic and non-systematic).

G	m	s	n	k	$n-k$	R_c	O_c	c	ρ	γ	J
systematic codes											
EG-2	5	1	248	217	31	0.875	14.3%	8	16	2	31
EG-2	6	1	504	441	63	0.875	14.3%	8	16	2	63
EG-2	7	1	1016	889	127	0.875	14.3%	8	16	2	127
EG-2	8	1	2040	1785	255	0.875	14.3%	8	16	2	255
EG-2	4	2	2040	1785	255	0.875	14.3%	8	32	4	255
EG-2	5	2	8184	7161	1023	0.875	14.3%	8	32	4	1023
EG-2	3	3	4088	3577	511	0.875	14.3%	8	64	8	511
EG-2	3	4	32760	28665	4095	0.875	14.3%	8	128	16	4095
EG-2	4	3	32760	28665	4095	0.875	14.3%	8	64	8	4095
PG-2	6	1	1016	889	127	0.875	14.3%	8	24	3	127
PG-2	7	1	2040	1785	255	0.875	14.3%	8	24	3	255
PG-2	8	1	4088	3577	511	0.875	14.3%	8	24	3	511
PG-2	4	2	2728	2387	341	0.875	14.3%	8	40	5	341
PG-2	5	2	10920	9555	1365	0.875	14.3%	8	40	5	1365
PG-2	3	3	4680	4095	585	0.875	14.3%	8	72	9	585
PG-2	3	4	34952	30583	4369	0.875	14.3%	8	136	17	4369
PG-2	4	3	37448	32767	4681	0.875	14.3%	8	72	9	4681
non-systematic codes											
EG-2	7	1	1016	890	126	0.876	14.2%	8	16	2	127
EG-2	8	1	2040	1786	254	0.875	14.2%	8	16	2	255
PG-2	4	3	32767	28676	4091	0.875	14.3%	7	63	9	4681

Table 9. Shortened type 2 EG and PG LDPC codes of about 15% overhead (systematic and non-systematic).

G	m	s	n	k	$n-k$	R_c	O_c	c	ρ	γ	J
non-systematic codes											
EG-2	4	2	1785	1551	234	0.869	15.1%	7	28	4	255
EG-2	4	3	28665	24976	3689	0.871	14.8%	7	56	8	4095
PG-2	5	1	441	384	57	0.871	14.8%	7	21	3	63

Table 10. Extended type 2 EG LDPC codes with various overhead.

G	m	s	n	k	$n-k$	R_c	O_c	c	ρ	γ	J
systematic, extended rows											
EG-2	4	2	5355	4845	510	0.905	10.5%	21	41	4	510
EG-2	5	2	32736	30690	2046	0.938	6.7%	32	63	4	1023
EG-2	5	2	86955	84909	2046	0.977	2.4%	85	169	4	1023
shortened, extended rows and extended columns											
EG-2	3	3	8176	7154	1022	0.875	14.3%	8	32	4	1022
EG-2	3	3	9198	8176	1022	0.889	12.5%	9	36	4	1022
systematic, extended rows and extended columns											
EG-2	3	3	8176	7154	1022	0.875	14.3%	8	31	4	1022
EG-2	3	3	9198	8176	1022	0.889	12.5%	9	35	4	1022